T1-A

International Journal of Modern Physics E
Vol. 15, No. 4 (2006) 853–863
© World Scientific Publishing Company

RELATIVISTIC TRANSPORT APPROACH TO THE NUCLEAR GROUND STATE

SERBULENT YILDIRIM
Fizik Bölümü, Mersin Üniversitesi, 33343 Mersin, Turkey
syildirim@mersin.edu.tr

Received 24 January 2006

The ground state properties of finite nuclei are studied in the framework of a relativistic transport approach. The kinetic equations are derived within an effective nucleon-meson field theory in the Relativistic Mean Field (RMF) scheme. The time evolution of the binding energies and the nuclear radii are obtained for spherical nuclei with various sets of Lagrangian parameters and compared with those of Relativistic RPA results for ^{208}Pb. The comparison shows reasonably well results.

1. Introduction

Both the relativistic and non-relativistic transport models have been extensively used to study heavy ion collisions (HIC)[1,2] and the collective dynamical properties of a single nucleon.[3,4] In these models the evolution of the one-body phase-space distribution of the colliding nuclei or a single nucleus is described by semi-classical transport equations of the Boltzmann type. These equations consist of a mean-field potential part where particles propagate and a collision part for the scattering of the particles. In the case of excluding or neglecting the collision part, one obtains the Vlasov equation. The one-body phase-space distribution function $f(r, p, t)$ entering the Vlasov equation is the Wigner transform of the one-body density matrix $\rho(r, p, t)$ which satisfies the Time Dependent Hartree Fock (TDHF) equation.[5,6] Although in HIC simulations one interests in the final state observables which are assumed or approximated to be independent of the initial configurations of the colliding nuclei, it has been pointed out that HIC simulation tests with different initial configurations show that some observables might be sensitive to the initialization of participants.[7] As it is evident from the definitions of the transport models, the most accurate way would be to generate the ground state configuration from the Wigner transform of a self-consisted solution for the ground state. But such a calculation is still missing in the literature.

The commonly used method to obtain the ground state of a nucleus is to represent the one-body phase-space distribution function in terms of the sum of elementary functions known as test particle ansatz, following Wong.[8] In general pointlike

test particles of the δ-functions or gaussian functions are chosen for both in coordinate and momentum space representations of the phase-space distribution function. For example, the initial configuration in position space, for the nucleus under consideration, is obtained by randomly distributing the test particles within a sphere of radius R. This radius is determined such that the single nucleus remains stationary for long enough time compare to the time scale of the physical property that is under investigation.

In this work we study the ground state properties of ^{208}Pb using the Relativistic Vlasov method (RV) in a Relativistic Mean Field (RMF) theory. We applied various RMF models with different coupling parameters which lead to a different nucleon effective mass (m^*), compressibility modulus (K_{nm}), symmetry energy (a_4), keeping fixed other nuclear matter saturation properties.

Among those models we focus on the ones where the scalar isovector channel has been introduced by the coupling to an effective δ-meson field.[9] It has been shown that such inclusion has important effects on the equation of state (EOS) and phase diagram of asymmetric nuclear matter (ANM), as well as on the reaction dynamics with exotic nuclei, see the review.[1] In fact the δ-meson brings contributions to the slope and curvature of the symmetry energy and to the neutron-proton effective mass splitting. In particular the influence of this coupling on the collective response of (ANM) appears important, as shown in a linear response approach in Ref. 10. For the comparison of the results we have also considered the well known NL3[11,12] parametrization, very successful for finite nuclei structure calculations. In this way we aim to pin down the sensitivity of the ground state properties focussing on the interplay between isoscalar-isovector couplings.

Relativistic mean field models, with constant[13,14] meson-nucleon couplings, have been applied to the description of ground state properties of atomic nuclei in the framework of the self-consistent relativistic random phase approximation (RRPA). In this respect we compare the relativistic Vlasov calculation results with the RRPA for the ground state in spherical n-rich nuclei.

2. Outline of the Model

The ground state of a spherical nuclei is studied in the framework of the relativistic Vlasov (RV) transport equation, which describes the dynamical evolution of a semi-classical phase space distribution function $f(x,p)$ under the influence of the nuclear mean field. Thorough derivations of the RV transport equations from an effective hadron-meson field theory,[15] can be found elsewhere.[5,16,17] The RV equation reads ($i = p, n$):

$$[p_i^{*\mu}\partial_\mu + (p^*_{\nu i}\mathcal{F}_i^{\mu\nu} + m_i^*\partial^\mu m_i^*)\partial_\mu^{(p_*)}]f_i(x,p^*) = 0 \tag{1}$$

with the field tensor

$$\mathcal{F}_i^{\mu\nu} \equiv \partial^\mu\Sigma_i^\nu - \partial^\nu\Sigma_i^\mu \tag{2}$$

and effective masses and kinetic momenta m^* and $p^{*\mu}$, respectively, specified below. The particles obey the mass-shell condition

$$p_i^{*\mu} p_{i\mu}^* - m_i^{*2} = 0\,. \tag{3}$$

Thus, from the temporal knowledge of the phase space distribution function one can calculate the time evolution of physical quantities such as densities and fields. We remind the meaning of the the Wigner matrix (in the Spinor space)

$$\begin{aligned} F_{\alpha\beta}(x,p) &= \langle \hat{F}_{\alpha\beta}(x,p)\rangle \\ &\equiv \frac{1}{(2\pi)^4}\int d^4\mathrm{Re}^{-ip_\mu R^\mu}\left\langle \bar{\psi}_\beta\left(x+\frac{1}{2}R\right)\psi_\alpha\left(x-\frac{1}{2}R\right)\right\rangle . \end{aligned} \tag{4}$$

From the above definition it follows that single-particle operators can be expressed as (spinor indices will be omitted for simplicity)

$$\langle \hat{O}\rangle = \int d^4x \int d^4p\,\mathrm{tr}(\hat{O}F(x,p)) \tag{5}$$

where the trace runs over spin and isospin indices. The scalar density and the vector current, for example, assume the form

$$\rho_s(x) = \langle \bar{\psi}\psi\rangle = \int d^4p\,\mathrm{tr}(F(x,p)) \tag{6}$$

$$j_\mu(x) = \langle \bar{\psi}\gamma_\mu\psi\rangle = \int d^4p\,\mathrm{tr}(\gamma_\mu F(x,p))\,, \tag{7}$$

and will be used to calculate the different Lorentz components of the mean field potential.

The nuclear mean field U is characterized in a RMF theory by means of self energies in the form $U = \Sigma_s - \gamma_\mu\Sigma^\mu\cdots$ (higher contributions are usualy neglected due to symmetry properties of nuclear matter). In a nonlinear (QHD-NL) model with isoscalar scalar and vector meson fields σ and ω and with the inclusion of the isovector channel through the exchange of the virtual charged δ (scalar) and ρ (vector) mesons, the mean field approximation leads to self energies which are related to the expectation values of the combination of isoscalar and isovector fields with coupling constants g_σ, g_ω, g_ρ and g_δ. The scalar and vector components of the self energies are generally given by

$$\Sigma_i^\mu = g_\omega\omega^\mu(x) \pm g_\rho b^\mu(x) \qquad \begin{cases} +\ \text{proton}(i=p) \\ -\ \text{neutron}\ (i=n) \end{cases} \tag{8}$$

$$\Sigma_{si} = g_\sigma\sigma(x) \pm g_\delta\delta(x) \qquad \begin{cases} +\ \text{proton}\ (i=p) \\ -\ \text{neutron}\ (i=n) \end{cases} \tag{9}$$

with the expectation values of the fields self-consistently calculated, see Eq. (19).

The self energies characterize the in-medium properties of the nucleons inside the hadronic environment in terms of kinetic momenta and effective masses

$$p_i^{*\mu} = p_i^\mu - \Sigma_i^\mu \tag{10}$$

Table 1. Coupling parameters in terms of $f_i \equiv (g_i/m_i)^2$ for $i = \sigma, \omega$, $f_i \equiv (g_i/2m_i)^2$ for ρ, δ, $A \equiv a/g_\sigma^3$ and $B \equiv b/g_\sigma^4$ for various nonlinear RMF models using the ρ and both ρ and δ mesons for the characterization of the isovector mean field. In the DDH models the coupling functions are explicitly density dependent.[18,20,22]

Parameter	NL1-G	NL2-G	NL3	NLρ	NL$\rho\delta$
$f_\sigma(fm^2)$	6.146	9.300	15.739	10.330	10.330
$f_\omega(fm^2)$	3.611	3.611	10.530	5.420	5.420
$f_\rho(fm^2)$	1.200	1.220	1.339	0.950	3.150
$f_\delta(fm^2)$	0.0	0.0	0.0	0.0	2.500
$A(fm^{-1})$	−0.123	0.0824	−0.01	0.033	0.033
B	0.169	−0.0012	−0.003	−0.0048	−0.0048

Table 2. Nuclear matter saturation properties in the different RMF models.

Property	NL1-G	NL2-G	NL3	NLρ, $\rho\delta$	DDHρ, $\rho\delta$
E/A (MeV)	−16.0	−16.0	−16.3	−16.0	−16.0
ρ_0 (fm^{-3})	0.145	0.145	0.148	0.160	0.153
$m^*/$m	0.83	0.83	0.60	0.75	0.55
K_{nm} (MeV)	380	210	272	240	240
a_4 (MeV)	30.62	30.62	37.40	30.50	33.40

$$m_i^* = m - \Sigma_{si} \,. \tag{11}$$

The density dependence of the mean field, i.e. the density behavior of the self energies, depends on the coupling choices of the RMF model. Here we consider different parametrizations within the nonlinear (QHD-NL) effective field approach. In Table 1 the values for the different coupling constants and the nonlinear parameters for different sets of nonlinear Walecka (QHD-NL) models are presented, for details see Refs. 1, 9–11 and 18. Their corresponding nuclear matter saturation properties are given in Table 2.

The choice of models with rather different nuclear matter properties has been done on purpose, in order to investigate the role of the effective masses, compressibility and symmetry energy on the ground state properties in neutron-rich nuclei. We have compared various nonlinear RMF parametrizations, in particular the Giessen sets NL1-G, NL2-G,[19] extended also to simulations of relativistic heavy ion collisions, and the widely used NL3 set,[11,12] successfully applied in finite nuclei studies. The different treatment of the iso-vector part of the mean field (competition effects of the repulsive ρ field and the attractive δ meson) is analyzed in detail using the (NLρ, NL$\rho\delta$) parameter sets.[9] The same analysis is performed within density dependent coupling models, the parametrizations DDH3ρ and DDH3$\rho\delta$ of Ref. 20 have been used.

The dynamics of ground state properties in spherical nuclei is simulated in the framework of the relativistic Vlasov equation (1). Its numerical realization is based

on the standard test particle method, where the phase space distribution function $f(x,p)$ is represented by a finite number of test particles of a covariant Gaussian form (Relativistic Landau-Vlasov (RLV) method). A detailed description of the RLV method is given in Ref. 21, this model will be briefly discussed here. The use of a Gaussian shape for the test particles has the advantage of smooth distribution functions, but maintaining an accurate determination of local quantities, particularly important near the nuclear surface.

The covariant Gaussians in the four-dimensional Minkowski space are defined as

$$\begin{aligned} G(x;\xi_i) &\equiv \int_{-\infty}^{-\infty} d\tau g(x - x_i(\tau)) \\ &= \alpha \int_{-\infty}^{-\infty} d\tau \exp((x - x_i(\tau))^2/w^2)\delta[(x_\mu - x_{i\mu}(\tau))u_i^\mu(\tau)] \end{aligned} \tag{12}$$

where ξ_i denotes the world line of the particle i as a whole, τ refers to the eigentime of the test particle and α is the normalization constant. In the four-dimensional momentum space a gaussian weight of a test particle is defined by[21]

$$g(p^* - p_i^*(\tau)) \equiv \alpha_p \exp((p^* - p_i^*(\tau))^2/w_p^2)\delta[p_\mu^* p_i^{*\mu}(\tau) - m_i^{*2}] \tag{13}$$

where the center of the gaussian is assumed to be on-shell i.e. $p_{i\mu}^* = m_i^* u_{i\mu}$, $u_i^2 = 1$, whereas the free momentum p_μ^* is generally off-shell. The effective mass of the particle is taken as $m_i^* = m^*(x_i(\tau))$. The norm of the gaussian is calculated in the rest frame of the particle to be m_i^{*-1} with $\alpha_p = (\sqrt{\pi} w_p)^{-3}$, where w and w_p are the test particle widths in position and momentum space.

With the gaussians of (12) and (13), the phase space distribution function $f(x,p^*)$ is expressed as

$$\begin{aligned} f(x,p^*) &= \frac{1}{N}\sum_{i=1}^{A\cdot N}\int_{-\infty}^{+\infty} d\tau g(x - x_i(\tau))g(p^* - p_i^*(\tau)) \\ &= \frac{1}{N(\pi w w_p)^3}\sum_{i=1}^{A\cdot N}\int_{-\infty}^{-\infty} d\tau \exp((x - x_i(\tau))^2/w^2) \\ &\quad \times \exp((p^* - p_i^*(\tau))^2/w_p^2) \\ &\quad \times \delta[(x_\mu - x_{i\mu}(\tau))u_i^\mu(\tau)]\delta[p_\mu^* p_i^{*\mu}(\tau) - m_i^{*2}] \end{aligned} \tag{14}$$

where N is the number of test particles per nucleon. Scalar densities ρ_s and baryon currents j_μ follow from the phase space distribution

$$\rho_s(x) = \frac{1}{N}\sum_{i=1}^{A\cdot N}\int_{-\infty}^{-\infty} d\tau \frac{m^*(x)}{m^*(x_i(\tau))} g(x - x_i(\tau)) \tag{15}$$

$$j_\mu(x) = \frac{1}{N}\sum_{i=1}^{A\cdot N}\int_{-\infty}^{-\infty} d\tau g(x - x_i(\tau))u_{i\mu}(\tau)\,. \tag{16}$$

The equations of motion for the test particle trajectories are given by

$$\frac{d}{d\tau}x_i^\mu(\tau) = u_i^\mu(\tau) \tag{17}$$

$$\begin{aligned}\frac{d}{d\tau}u_i^\mu(\tau) = {} & \frac{1}{m^*(x_i)}\sum_{j=1}^{A\cdot N}\frac{2}{w^2}\left[\frac{g_\omega^2}{m_\omega^2}u_{i\nu}(R_j^\mu(x_i)u_j^\nu - R_j^\nu(x_i)u_j^\mu)\right. \\ & \left. - g_\sigma\frac{\partial\sigma(x_i)}{\partial\rho_s}(R_j^\mu(x_i) - u_i^\mu u_i^\nu R_{j\nu}(x_i))\right]\frac{\exp(R_j^2(x_i)/w^2)}{N(\sqrt{\pi}w)^3} \\ & \pm\frac{1}{m^*(x_i)}\frac{2}{w^2}\sum_{j=1}^{Z\cdot N}\left[\frac{g_\rho^2}{4m_\rho^2}u_{i\nu}(R_j^\mu(x_i)u_j^\nu - R_j^\nu(x_i)u_j^\mu)\right. \\ & \left. - \frac{g_\delta^2}{4m_\delta^2}u_{i\nu}(R_j^\mu(x_i) - u_i^\mu u_i^\nu R_{j\nu}(x_i))\right]\frac{\exp(R_j^2(x_i)/w^2)}{N(\sqrt{\pi}w)^3} \\ & \mp\frac{1}{m^*(x_i)}\frac{2}{w^2}\sum_{j=Z\cdot N+1}^{A\cdot N}\left[\frac{g_\rho^2}{4m_\rho^2}u_{i\nu}(R_j^\mu(x_i)u_j^\nu - R_j^\nu(x_i)u_j^\mu)\right. \\ & \left. - \frac{g_\delta^2}{4m_\delta^2}u_{i\nu}(R_j^\mu(x_i) - u_i^\mu u_i^\nu R_{j\nu}(x_i))\right]\frac{\exp(R_j^2(x_i)/w^2)}{N(\sqrt{\pi}w)^3}\end{aligned} \tag{18}$$

with

$$R_i^\mu(x) \equiv (x^\mu - x_i^\mu(\tau)) - (x_\nu - x_{i\nu}(\tau))u_i^\nu(\tau)u_i^\mu(\tau)\,,$$

projection of the vector $(x - x_i(\tau))$ on the hyperplane perpendicular to $u_i(\tau)$.[21]

Here the equations for velocities, rather than for momenta, are given, within the assumption that the particle accelerations are small. In this equation particles are propagated by their respective eigentimes and so corresponding time coordinates $x_{i0}(\tau)$ can differ. In order to solve the problem of different time coordinates a *system time* has been adopted for the propagation.[21]

The scalar and vector meson fields, determined by the scalar density ρ_s and the baryonic current j_μ, respectively, result from the solution of the corresponding equations in the Local Density Approximation (LDA)

$$\begin{aligned} m_\sigma^2\sigma(x) + B\sigma^2(x) + C\sigma^3(x) = g_\sigma\rho_s(x) &\equiv g_\sigma\int d^4p^*\frac{m^*(x)}{E^*(x)}f(x,p^*) \\ \omega_\mu(x) = \frac{g_\omega}{m_\omega^2}j_\mu(x) &\equiv \frac{g_\omega}{m_\omega^2}\int d^4p^*p_\mu^*f(x,p^*) \\ b_\mu(x) = \frac{g_\rho}{4m_\rho^2}j_{3\mu}(x) &\equiv \frac{g_\rho}{4m_\rho^2}\int d^4p^*p_\mu^*f_3(x,p^*) \\ \delta(x) = \frac{g_\delta}{4m_\delta^2}\rho_{s3}(x) &\equiv \frac{g_\delta}{4m_\delta^2}\int d^4p^*\frac{m^*(x)}{E^*(x)}f_3(x,p^*)\,. \end{aligned} \tag{19}$$

with $f_3 \equiv f_p - f_n$.

An important issue for the description of nuclear ground state within the RV equation is an appropriate initialization of finite nuclei, before starting the phase space evolution of the distribution function with Eq. (18). The ground state of a spherical nucleus is randomly initialized by means of the test particles with the covariant gaussian shape in position and momentum space. After the first step of a randomly obtained initial distribution, a fit procedure in coordinate space is performed according to realistic Thomas–Fermi reference density distributions. During this procedure the proton and neutron distributions are fitted separately by satisfying the empirical values for the asymmetry and the surface thickness parameters, respectively. In the Thomas–Fermi calculation the scalar densities are determined by solving self-consistently the equations for the effective masses $m^*_{p,n}$. With this initialization of a given spherical nucleus the temporal evolution is described by the RLV equation (18). We have used 100 test particles per nucleon for the transport descriptions, which yields a smooth distribution function with a very good energy conservation.

3. Results and Discussion

The first observation in the initialization is to decide the widths of gaussians in position or momentum space. Since they are related by the minimum uncertainity relation $\sigma_x \sigma_p = \hbar/2$ it is enough to decide one of them. Here we consider the σ_x width in position space. There is no way from the formalism to decide its value. In the literature[21] the gaussian in momentum space is interpreted as an approximation to the spectral function of the particles and for the width of the spectral function the self energies from Dirac–Brueckner calculations is taken[23] and compared to the gaussian parametrization in the rest frame of the particle. The fit for the value of σ_p for a particle with a mean momentum of $p_i = 650$ MeV in nuclear matter of density 3/2 times the saturation density for the compression phase in a heavy-ion collision is found to be $\sigma_p = 0.4$ fm^{-1} which corresponds to $\sigma_x = 1.25$ fm ($\hbar = 1$). Since this value of σ_x obtained for the HIC case in a larger nuclear density, we tune this value for the ground state of ^{208}Pb by directly observing its effect on the stability of ground state. For this reason we work for different values of σ_x from 0.8 fm to 1.4 fm. The results are shown in Fig. 1. Where we see that the stabilty increases significantly as we go from 0.8 fm value to 1.35 fm for σ_x and start to lose the stability after that value as we reach $\sigma_x = 1.4$ fm. Of course there are no dynamical reasons from the equation of motion for this result, but is has to be from numerical origin related to the packing of gaussians in to a finite space to get a certain density distribution over nuclear radius.

After deciding the width of gaussians now we can turn to find the relativistic mean field parametrization that produce the most stable ground state and an experimentally correct rms radius and binding energy. For this reason we have applied the model parameters in Table 1 for which the nuclear matter properties of the model parameters are shown in Table 2. The results of the time evaluation of

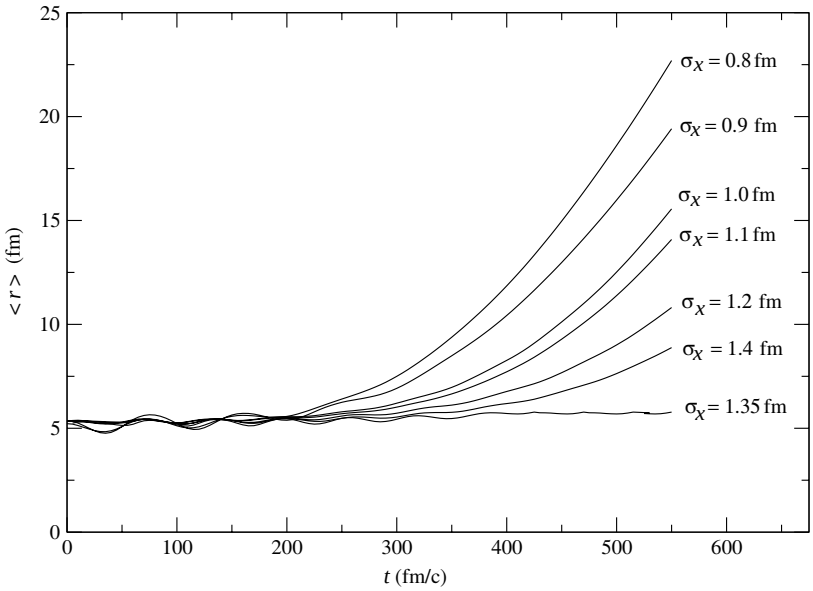

Fig. 1. The time evaluation of ground state rms radius of ^{208}Pb for different σ_x values.

the ground state rms radius and the average value over time $\langle r \rangle$ and the average binding energy per nucleon $\langle E \rangle$ are shown in Fig. 2. The first observation in the ground state properties is that the contribution of delta meson is negligible. So the nonlinear parametrization of NLρ and NL$\rho\delta$ gives the same ground state properties. We also observe that the density dependent model DDH is also producing very similar results to NLρ. We show them in the down-right panel in Fig. 2. In general we see that all the model parameters produce very similar rms radius and binding energy per nucleon. The success of NL3 parametrization in producing the binding energy per nucleon with the RPA results of Ref. 12 and the most close value to the experimental rms radius of value is striking. Although the general behavior of the time evaluation of rms radius show similar behavior, the oscilation amplitude and frequency change among models. The lowest oscillation amplitude and highest frequency of NL1-G (upper right panel) and largest oscillation amplitude of NL2-G (lower left panel) are attributed to the compressibility of the corresponding models namely NL1-G being the highest (380 MeV) and NL2-G being the lowest (210 MeV). The other models (NL3, NLρ) having a comparatively close compressibility values (272 MeV, 240 MeV) being between NL1-G and NL2-G parametrization show a behavior somehow in between these two extreme cases. For a detailed discussion for the relation between compressibility and nuclear monopole oscillations see Ref. 3.

In order to watch the stability in detail we show the time evaluation of the proton-neutron and total density starting from the beginning and taking a snapshot

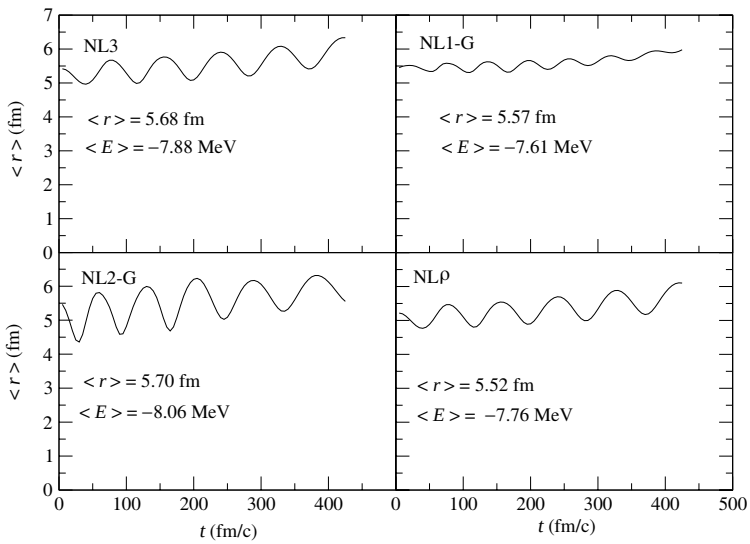

Fig. 2. The time evaluation of the ground state rms radius and calculated average ground state energy ($\langle E \rangle$) and average rms radius of ($\langle r \rangle$) ^{208}Pb for different RMFT coupling parameter sets.

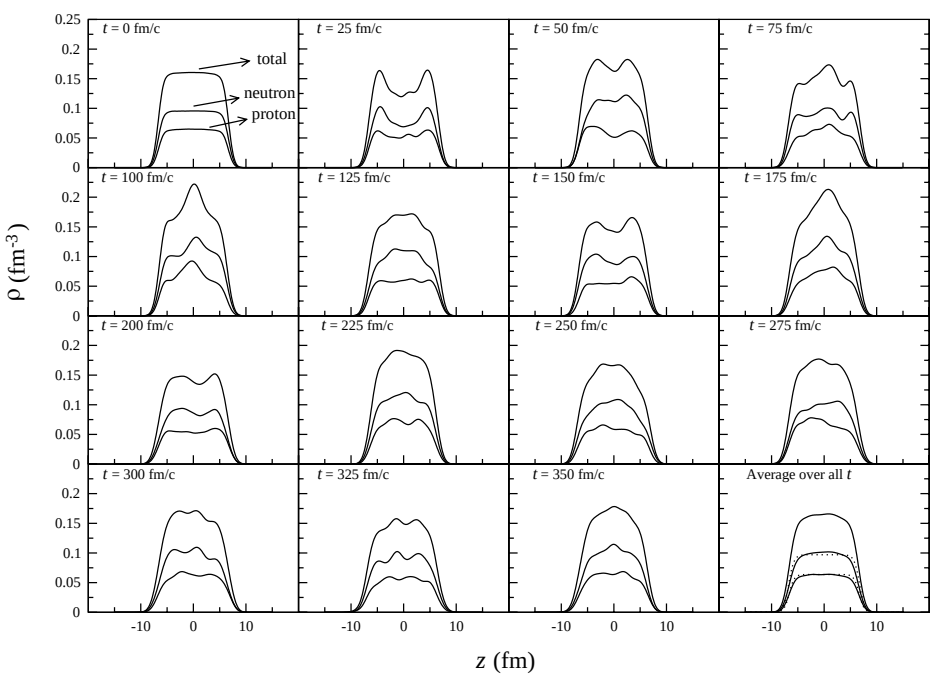

Fig. 3. The snapshots of the proton-neutron and total density at every 25 fm/c starting from the beginning (panel 1.1) and up to 350 fm/c (panel 4.3), and the average of all densities over all time steps and compared to the initial distributions (initial distributions is shown with dotted lines, panel 4.4).

of every 25 fm/c up to 350 fm/c in Fig. 3. At the end, we average the densities over all time steps and make a comparison with initial distributions. We observe that except a small increase in central part of the neutron distribution we obtain a steady ground state.

4. Conclusions

Aim of this work has been to study the properties of the ground state of spherical nuclei in a relativistic transport approach based on a nucleon-meson effective field interaction. We have evaluated the time-evolution of the ground state obtaining its stability, energy and rms radius. Effects of different RMFT parametrization sets on the properties of spherical nuclei ^{208}Pb are studied in detail for both in the isoscalar and isovector sector. Particular attention has been put on the dynamical implications of the inclusion of a scalar isovector contribution due to an effective δ meson coupling. But no significant contribution is found for the ground state n-rich ^{208}Pb nuclei. Although all the parameter sets show similar ground state dynamical behavior the NL3 paramtrization is shown to be the RMF parameter set that produce the most stable ground state and the most accurate ground state energy and rms radius results very close to the values obtained by RRPA results. Finally we do not see large effects from the Density Dependence of the effective meson couplings and we obtained same ground state properties as NL-ρ set.

Acknowledgments

This work has been supported by Mersin University under the contract No. BAB FEF FB (SY) 2004-2, and we are grateful to Mr. Turgut GUR for his computer support to the Physics Department.

References

1. V. Baran, M. Colonna, V. Greco and M. Di Toro, *Phys. Rep.* **410** (2005) 335–466 and references therein.
2. T. Gaitanos, M. Di Toro, S. Typel, V. Baran, C. Fuchs, V. Greco and H. H. Wolter, *Nucl. Phys. A* **732** (2004) 24.
3. S. Yildirim, T. Gaitanos, M. Di Toro and V. Greco, *Phys. Rev. C* **72** (2005) 064317.
4. K. Morawetz, U. Fuhrmann and R. Walke, *Collective Modes in Asymmetric Nuclei Chapter of Isospin Book*, ed. B.-A. Li (World Scientific, 2000).
5. B. Blaettel, V. Koch and U. Mosel, *Rep. Prog. Phys.* **56** (1993) 1.
6. A. Bonasera, F. Gulminelli and J. Molitoris, *Phys. Rep.* **243** (1994) 1.
7. B. Blättel, V. Koch, W. Cassing and U. Mosel, *Phys. Rev. C* **38** (1988) 1767.
8. C. Y. Wong, *Phys. Rev. C* **25** (1982) 1460.
9. B. Liu, V. Greco, V. Baran, M. Colonna and M. Di Toro, *Phys. Rev. C* **65** (2002) 045201.
10. V. Greco, M. Colonna, M. Di Toro and F. Matera, *Phys. Rev. C* **67** (2003) 045201.
11. P. Ring, D. Vretenar and B. Podobnik, *Nucl. Phys. A* **598** (1996) 107.
12. G. A. Lalazissis, J. Konig and P. Ring, *Phys. Rev. C* **55** (1997) 540.

13. M. V. Stoitsov, P. Ring and M. M. Sharma, *Phys. Rev. C* **50** (1994) 1445.
14. D. Vretenar, N. Paar, P. Ring and T. Niksic, *Phys. Rev. C* **65** (2002) 021301.
15. B. D. Serot and J. D. Walecka, *Adv. Nucl. Phys.* **16** (1986) 1.
16. W. Botermans and R. Malfliet, *Phys. Rep.* **198** (1990) 115.
17. P. Danielewicz, *Ann. Phys.* **152** (1984) 239.
18. S. Typel and H. H. Wolter, *Nucl. Phys. A* **656** (1999) 331.
19. T. Maruyama, W. Cassing, U. Mosel, S. Teis and K. Weber, *Nucl. Phys. A* **573** (1994) 653.
20. T. Gaitanos, M. Di Toro, S. Typel, V. Baran, C. Fuchs, V. Greco and H. H. Wolter, *Nucl. Phys. A* **732** (2004) 24.
21. C. Fuchs and H. H. Wolter, *Nucl. Phys. A* **589** (1995) 732.
22. C. Fuchs, H. Lenske and H. H. Wolter, *Phys. Rev. C* **52** (1995) 3043.
23. B. ter Haar and R. Malfliet, *Phys. Rep.* **149** (1987) 207.